IJIE

UTHM Penerbit

INTERNATIONAL JOURNAL OF INTEGRATED ENGINEERING
ISSN: 2229-838X e-ISSN: 2600-7916

Vol. 18 No. 3 (2026) 147-165
https://publisher.uthm.edu.my/ojs/index.php/ijie

Parametric Analysis and Optimization on Aerodynamic Performance of Optimized Pedestrian Crash Friendly Sedan Front End Profiles

Afzatul Najwa Nor Azman[1], Kausalyah Venkatason[1]*, Shasthri Sivaguru[2]

[1] *School of Mechanical Engineering, College of Engineering, Universiti Teknologi MARA, 40450 Selangor Darul Ehsan, MALAYSIA*
[2] *School of Engineering & Physical Sciences, Heriot Watt University Malaysia, Precinct 5, Putrajaya, 62200 Wilayah Persekutuan Putrajaya, MALAYSIA*

*Corresponding Author: kausalyah@uitm.edu.my
DOI: https://doi.org/10.30880/ijie.2026.18.03.010

Article Info

Received: 23 March 2025
Accepted: 14 December 2025
Available online: 30 April 2026

Keywords

Vehicle Front-End (VFE), Central Composite Design (CCD), Genetic Algorithm (GA), Computational Fluid Dynamics (CFD), Head Injury Criterion (HIC)

Abstract

This paper offers a multi-objective optimization framework balancing aerodynamic efficiency with pedestrian safety in Vehicle Front-End (VFE) design. While lowering the Head Injury Criterion (HIC) to lower pedestrian injury risks in crashes, the aim is to minimize the drag coefficient (Cd) for enhanced fuel economy and vehicle dynamics. Seven main design parameters such as windshield angle, hood edge height, and bumper centre height were investigated using a Central Composite Design (CCD) technique on Cd and HIC. Using MATLAB's MBC toolbox, response surface models were created; optimization was done using Genetic Algorithms (GA) in MATLAB's Solver-Based Optimize Live Editor Task. A successful predictive modelling was ensured by the fitness function, which maximized the R2 value (89.2% for Cd and 81.7% for HIC) and minimized the root mean square error (RMSE) (0.0065 for Cd and 0.01 for HIC). The optimal model was able to obtain a Cd of 0.1908 and an HIC of 99.7241, respectively, out of the total of 79 different VFE design alternatives that were developed. Computational fluid dynamics (CFD) validation using ANSYS yielded an 11.74% error within allowable engineering tolerance a simulated Cd of 0.2132. The results show the great relevance of hood edge height and windshield angle in order to increase aerodynamics and pedestrian safety. This work shows the effectiveness of incorporating evolutionary optimization, CFD, and safety analysis, so establishing a logical trade-off strategy for VFE design that enhances both aerodynamic performance and pedestrian protection.

1. Introduction

Road traffic accidents continue to be a major cause for concern since they cause so many injuries and deaths on a global scale. The World Health Organization (WHO) estimates that pedestrians contribute to more than a third of the 1.2 million yearly road traffic deaths globally, with many of them receiving serious multi-system injuries [1]. In Malaysia, children are particularly vulnerable as pedestrians rank third in road deaths, after cars and motorcycles. Studies show that youngsters between the ages of 6 and 10 account for a sizable fraction of pedestrian crash victims; their lower body size and altered post-impact kinematics cause often higher injury severity [2]. This combination of global and national data underscores the urgent need for design improvements that address pedestrian protection in the Malaysian context. One particularly deadly scenario is a 'run over' situation, where a child is knocked down and then run over instead of being thrown aside [3]. Since frontal vehicle crashes cause over 84% of pedestrian fatalities, the design of a vehicle's front end plays a crucial role in mitigating injury severity [4].

The vehicle's front-end geometry critically influences pedestrian safety by affecting impact dynamics such as head impact speed, angle, and point of contact [4, 5]. Therefore, optimizing front-end design to minimize the Head Injury Criterion (HIC), which is a standard indicator of head injury severity, is essential for reducing pedestrian injuries. Most existing research tends to rely on simplified rigid-body models, which limits its applicability to real-world collision situations [6, 7]. Regulatory measures and design advancements have improved safety, but many studies overlook the complex interactions among design features, emphasizing the need for a multi-objective optimization approach.

In addition to pedestrian safety, aerodynamics, represented by the drag coefficient (Cd), is vital for vehicle performance, affecting stability and fuel efficiency [8]. Aerodynamic modifications, such as sloped hoods, may reduce drag but can negatively influence pedestrian safety. Few studies address the trade-offs between aerodynamics and safety, often treating them independently [6, 7]. This discrepancy emphasizes the importance of an integrated design strategy that strikes both goals.

Optimizing vehicle front-end geometry is a challenging multi-objective task because design factors, aerodynamic performance, and pedestrian safety measurements are non-linear and interdependent. Traditional parametric studies frequently overlook variable interactions, and simplified modelling approaches (e.g., multi-body dynamics) do not fully capture vehicle deformation during impact. Combining Central Composite Design (CCD) with Genetic Algorithms (GA) allows for accurate representation of parameter interactions, enabling optimization that reduces drag and pedestrian injury risk.

The aerodynamic and safety performance of various vehicle front-end designs is evaluated in this work using computational fluid dynamics (CFD). Seven primary design parameters, which are windshield angle, bumper lead, bumper centre height, hood leading edge, hood length, hood angle, and hood edge height, were examined in MATLAB and ANSYS simulations to determine their effects on Cd and HIC. The solver based Optimize Live Editor task in MATLAB is used in the optimization process to provide an optimal front-end profile. This work intends to provide a new vehicle design process that improves both performance and crashworthiness by balancing aerodynamic efficiency with pedestrian safety issues. The results offer a more complete approach to vehicle front-end optimization, therefore helping to close the distance between aerodynamics and pedestrian safety.

2. Methodology

This paper suggests a multi-objective optimization framework to make the sedan front-end profiles better by increasing aerodynamic performance and lowering the risk of pedestrian head injuries at the same time. The overall method is organized into three distinct phases: modelling, optimization, and validation. Phase one is centered on creating geometric representations of the vehicle designs using Central Composite Design (CCD) sampling that can take place while developing the vehicle model's geometry, allowing for an efficient search of the design space.

2.1 Central Composite Design (CCD) Sampling Objective Function Generation

Mathematical modelling phase of this research has employed the Central Composite Design (CCD) Sampling to generate the computational experimental runs. CCD sampling was used as it facilitates designing speed while building the geometry of the vehicle models. The Model Based Calibration (MBC) Model Fitting toolbox, specifically focuses on the design of experiment portion, where a single-factor approach is selected. The number of components, fixed at 7, corresponds to the seven parameters that define the front-end profiles. Afterwards, the minimum and maximum parameter values are entered, taking into consideration the corresponding minimum and maximum values for each parameter.

In order to generate response model for the drag coefficient (Cd) and Head Injury Criterion (HIC), the data is inserted to the MBC Model toolbox. A polynomial subclass of the linear model class is chosen with an interaction order of 2.

Table 1 *Model setup for response model*

Model class:	Liner models
Linear model subclass:	Polynomial
	Order
x_1	2
x_2	2
x_3	2
x_4	2
x_5	2
x_6	2
x_7	2

Following the completion of the model's configuration, which is illustrated in Table 1, the objective function is produced in the model definition section. A desired low RMSE value and high R^2 is deemed acceptable to represent the objective function.

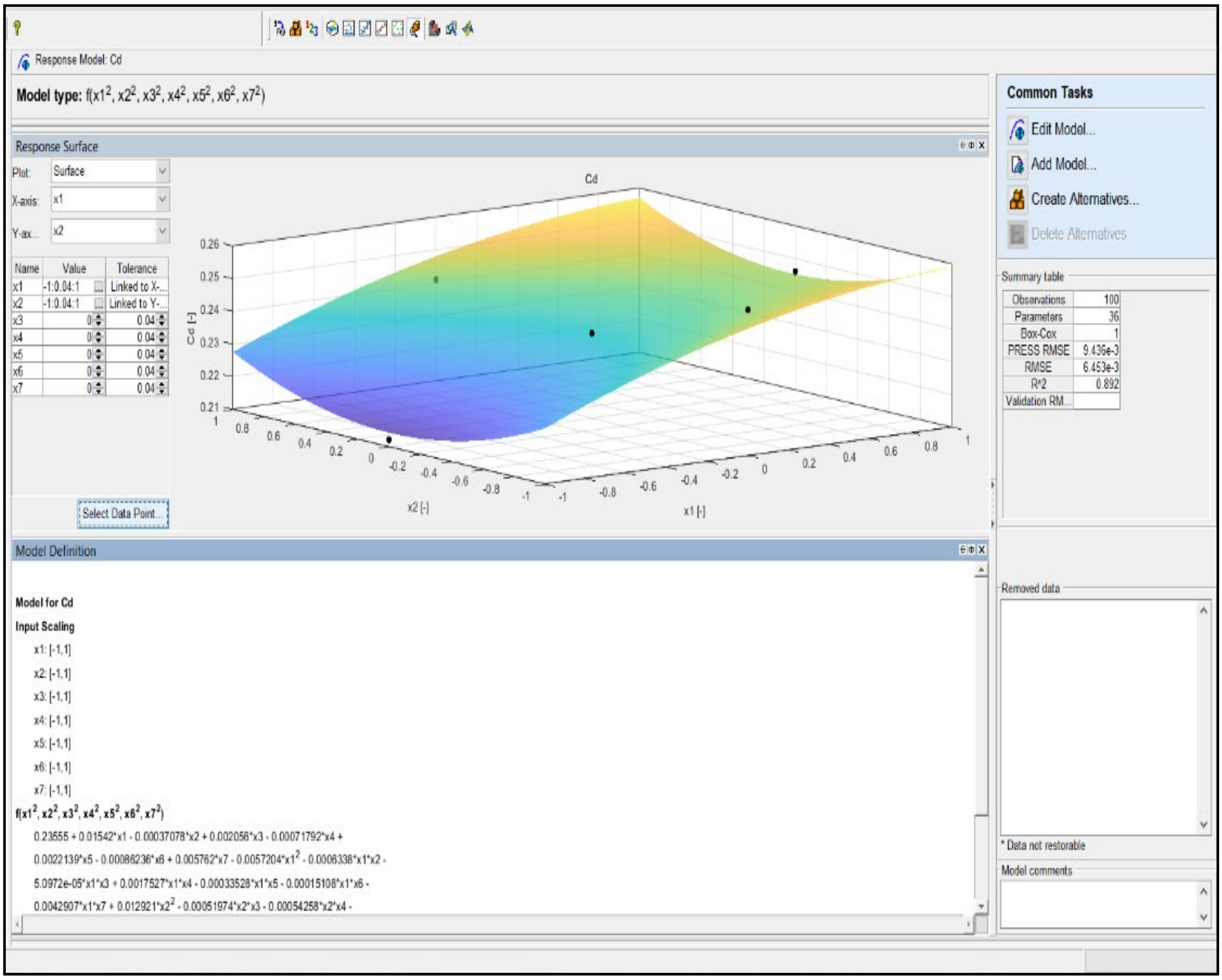

Fig. 1 *Response model using MBC toolbox*

The response model in Figure 1 shows a sample illustration of the interaction that occurs between two characteristics of the front end of the car. At the end of this response model, a fitness function will be generated.

2.2 VFE Significant Parameter Identification

This study focuses on identifying the parameters that contribute to the aerodynamic performance in the vehicle design. These vital frontal dimensions were selected based on previous studies where the vehicle front-end's profile was investigated for its safety in pedestrian impact [9, 10]. Seven key parameters related to modelling the frontal geometry of vehicles were included in these dimensions: bumper lead (BL), bumper center height (BCH), hood leading edge (HLE), hood length (HL), windshield angle (WSα), hood angle (Hα) and hood edge height (HEH). An illustration of these seven parameters is presented in Figure 2, which depicts the components required for analysis and the parametric description is shown in Table 2.

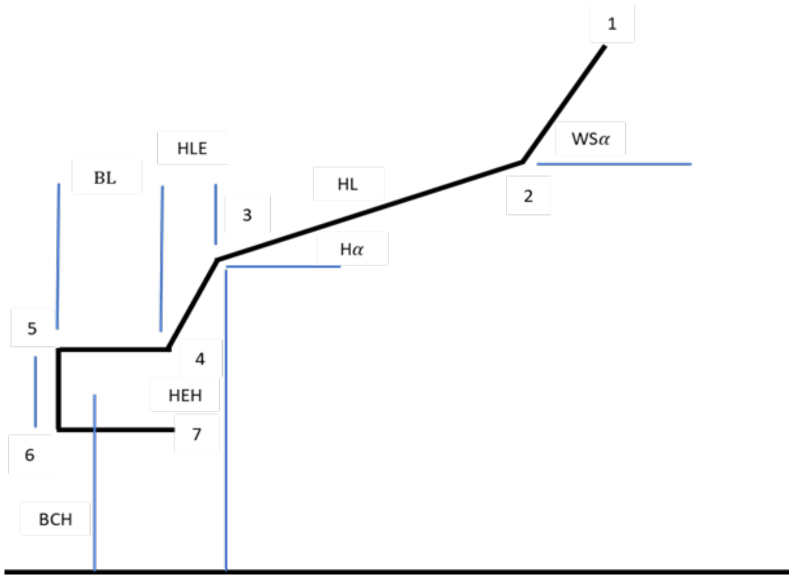

Fig. 2 *Seven parameters of sedan vehicle*

Table 2 *Parameter table (mm, degrees)*

x	Parameter	
x_1	WSα (Degrees)	Windshield Angle
x_2	BL	Bumper Lead
x_3	BCH	Bumper Centre Height
x_4	HLE	Hood Leading Edge
x_5	HL	Hood Length
x_6	Hα (Degrees)	Hood Angle
x_7	HEH	Hood Edge Height

Statistical investigations are then performed to determine which features have the most influence on aerodynamics performance, so that these parameters can be analysed effectively. A summary of these parameters is shown in Table 3, along with the uncoded values (mm or degrees), minimum, median, and maximum extents. This is the basis of the CCD methodology where the model with parameter interactions can be used to effectively expedite the design process.

Table 3 *Uncoded Parameter Analysis: Minimum, Median, and Maximum Values*

Parameter	x_1 (degrees)	x_2 (mm)	x_3 (mm)	x_4 (mm)	x_5 (mm)	x_6 (degrees)	x_7 (mm)
Minimum	29	10	435	50	635	11	565
Median	34.5	30	475.5	100	917.5	14.5	702
Maximum	40	50	516	150	1200	18	839

In the CCD framework, coded values of −1, 0, and 1 are given to the minimum, median, and maximum values of these parameters, respectively. For instance, x_1 (windshield angle) has uncoded values from 29 mm (minimum) to 40 mm (maximum), and a median of 34.5 mm. These coded values streamline the process of designing and analysing the experiment without losing precision.

2.3 VFE Multi-objective Optimization

The optimization approach aims to reduce drag coefficient (Cd) while maintaining pedestrian safety by minimizing head injury criterion (HIC). The multi-objective optimization strategy employs genetic algorithms (GA) to effectively address complicated optimization problems that traditional approaches could find challenging, by striking a balance between conflicting objectives.

The main goals of optimizing the VFE are to minimize the drag coefficient (Cd) to enhance fuel efficiency and vehicle dynamics, and to minimize the Head Injury Criterion (HIC) to decrease the possibility of injury in the event of a collision with a pedestrian in low impact speeds [9]. With the goal to accomplish these objectives, mathematical objective functions for the drag coefficient (Cd) and the Head Injury Criterion (HIC) are developed. The models are expressed as mathematical functions of the VFE design variables and subsequently translated into MATLAB code.

Genetic algorithms (GA) are selected for their resilience in addressing multi-objective optimization problems. Genetic algorithms (GAs) mimic the natural process of evolution by using techniques such as selection, crossover, and mutation to improve solutions across multiple generations [11]. The formulae for Cd and HIC are implemented in MATLAB. These functions are stored for use by the evolutionary algorithm in the Solver-Based Optimize Live Editor Task in MATLAB R2021a. In addition, the MATLAB workspace defines the number of design variables (nVar) and their corresponding boundaries (lower bound and upper bound).

The Solver-Based Optimize Live Editor Task in MATLAB is utilized to configure and solve the multi-objective optimization problem [12]. The goal function is configured as nonlinear by utilizing the objective function file that was created before. Additionally, the constraints are established by specifying the lower and upper boundaries for each design variable. The genetic algorithm is employed to choose the solver for multi-objective optimization.

The optimization work is set up and performed within the MATLAB environment. The Solver-Based Optimize Live Editor Task utilizes the genetic algorithm to achieve a balance between minimizing Cd (drag coefficient) and HIC (head injury criterion), leading to a collection of Pareto optimal solutions that demonstrate the trade-offs between aerodynamic efficiency and pedestrian safety. The solutions are subsequently examined to determine the optimal compromise design for the VFE [13].

multiobjective_optimization.m | boundariescoded.m | GetStartedWithOptimizeLiveEditorTaskExample14.mlx

```
function Output = multiobjective_optimization(Input)

%y(1)---Objective 1---equation for Cd minimize
%y(2)---Objective 2---equation for HIC minimize

% x(1)---Windshield Angle
% x(2)---Bumper Lead
% x(3)---Bumper Centre Height
% x(4)---Hood Leading Edge
% x(5)---Hood Length
% x(6)---Hood Angle
% x(7)---Hood Edge Height

x(1) = Input(1);
x(2) = Input(2);
x(3) = Input(3);
x(4) = Input(4);
x(5) = Input(5);
x(6) = Input(6);
x(7) = Input(7);

%Cd
y1 = 0.27764 + 0.014721*x(1) + 0.0022106*x(2) - 0.0084136*x(6) + 0.0023406*(x(1)*x(5

%HIC
y2 = 1.1962 + 0.055135*x(3) + 0.021726*x(4) + 0.11265*x(5) - 0.071624*(x(1)^2) + 0.0

Output = [y1 y2];
```

Fig. 3 *MATLAB coding setups*

The code for the objective function utilized in the multi-objective optimization process is depicted in Figure 3. Accurately configuring this code is essential for executing the optimizer in MATLAB, as any mistakes might have a substantial impact on the outcomes. Consequently, this procedure requires meticulous attention and accuracy.

The fitness function integrates both objective functions while maintaining the consistency of variables and parameters. This guarantees that the optimization process precisely mirrors the original design objectives for enhancing aerodynamic performance and pedestrian safety. The integrity of this coding step is crucial for the optimizer to operate accurately and generate dependable outcomes.

The MATLAB Workspace specifies the limits of the design space and the count of design parameters applied throughout the optimization process. The design vector shows as:

$$x = \{x_1, x_2, x_3, x_4, x_5, x_6, x_7\} \quad (1)$$

With constraints expressed as:

$$1 \leq x_i < 1\,, \quad \forall i \in \{1, 2, 3, 4, 5, 6, 7\} \quad (2)$$

where the arrays for lower bound (LB) and upper bound (UB) specify the allowed range for each parameter, making sure that the optimizer stays inside the range of $[-1, 1]^7$. The equation $n_{var} = 7$ represents the total number of design parameters. Encoding the variables inside this normalized range helps the optimization process to keep consistency over all parameters and increase computational efficiency. The optimizer in MATLAB is directed to investigate only viable solutions within the specified design space by these limitations.

2.4 Best Model Identification

The optimization process commences once the significant parameters are identified with the aim to identify the optimal model that effectively meets the defined objectives. This process entails the application of optimization algorithms or approaches to identify the most favorable allocation of parameter values that effectively enhance both aerodynamic performance and pedestrian safety concurrently. The optimization method entails examining a design space that is defined by the spectrum of parameter values with the goal to identify the most effective design.

During this phase, a thorough analysis and evaluation are carried out to ensure that the optimized VFE design effectively meets the defined objectives. The results obtained from the optimization process offer valuable insights into the balance between aerodynamic performance and pedestrian safety, enabling informed decision-making when choosing the final design. This phase sets the foundation for further enhancement and fine-tuning of the sedan's front-end profiles, resulting in exceptional performance across various objectives.

2.5 Validation of Optimized Model

For the purpose of verifying the optimized Vehicle Front-End (VFE) model that satisfies the aerodynamic and safety objectives that were established during the optimization process, the validation process is carried out. For the first step, the optimum design parameters are transformed into a three-dimensional model in CATIA V5 by making use of the real dimensions. This ensures that the simulation will be accurate. The next step is to generate a mesh in ANSYS, followed by a refinement study, with the goal of achieving a balance between accuracy and computation time. The simulation of the airflow around the vehicle is carried out with the help of computational fluid dynamics (CFD), and the drag coefficient (Cd) is compared to the target that has been optimized. In the case the values coincide, the aerodynamic performance of the model is acknowledged.

3. Result and Discussion

3.1 Central Composite Design (CCD) Sampling

Using three crucial metrics as shown in Table 4, observations, RMSE for Root Mean Squared Error, and R-squared (R^2), the MATLAB model fitting approach for a linear model polynomial response surface method produced significant discoveries.

The analysis employed 100 data point runs to train the model. It is beneficial to have such a large dataset since it provides the model with a large amount of information upon which to learn, hence enhancing its robustness and accuracy. Moreover, the root means square error (RMSE), which measures the differences between predicted and actual values, yielded a value of 0.0065 for Cd and 0.01 HIC. The low RMSE score denotes close agreement between the model's predictions and observed values, on average. Consequently, both models showed a high degree of accuracy in capturing each of the variations observed in the dataset [14].

Eventually, the R-squared (R^2) statistic, which indicates how much variance in the dependent variable (output) can be accounted for by the independent variables (input) in the model, had a value of 0.892 for Cd and 0.817 for HIC respectively. These scores for the coefficient of determination (R^2) indicates that the independent variables utilised in the model is capable of explaining about 89.2% and 81.7% of the variability in the dependent variable for each model.

Table 4 *Summary table for Cd and HIC*

Response Model	Drag Coefficient	HIC
Observations	100	100
Parameters	36	36
Box-Cox	1	1
PRESS RMSE	0.0094	0.145
RMSE	0.0065	0.01
R^2	0.892	0.817

Following the utilisation of the MBC model toolbox within MATLAB, the objective function that was produced is presented in equation below.

Drag coefficient (Cd) objective function:

$$y1 = 0.23555 + 0.01542\, x_1 - 0.00037078\, x_2 + 0.002056\, x_3 - 0.00071792\, x_4 + 0.0022139\, x_5 - 0.00086236\, x_6 + 0.005762\, x_7 - 0.0006338\, x_1x_2 - 0.00005097\, x_1x_3 + 0.0017527\, x_1x_4 - 0.00033528\, x_1x_5 - 0.00015108\, x_1x_6 - 0.0042907\, x_1x_7 - 0.00051974\, x_2x_3 - 0.00054258\, x_2x_4 - 0.000037634\, x_2x_5 - 0.00047638\, x_2x_6 - 0.00082267\, x_2x_7 - 0.00088615\, x_3x_4 + 0.0010497\, x_3x_5 + 0.000885\, x_3x_6 - 0.0032283\, x_3x_7 - 0.00043491\, x_4x_5 - 0.00071972\, x_4x_6 - 0.00057204\, x_4x_7 - 0.0013632\, x_5x_6 - 0.0010402\, x_5x_7 - 0.00060376\, x_6x_7 - 0.0057204\, x_1^2 + 0.012921\, x_2^2 - 0.0054718\, x_3^2 + 0.0038889\, x_4^2 + 0.0019623\, x_5^2 - 0.003140\, x_6^2 - 0.0011771\, x_7^2 \quad (3)$$

Head Injury Criteria (HIC) objective function:

$$y2 = 1.1932 + 0.014643\, x_1 - 0.015179\, x_2 + 0.055135\, x_3 + 0.021726\, x_4 + 0.11265\, x_5 + 0.015559\, x_6 + 0.0030687\, x_7 - 0.015524\, x_1x_2 - 0.0069287\, x_1x_3 - 0.0052815\, x_1x_4 - 0.0039343\, x_1x_5 + 0.0019329\, x_1x_6 - 0.0063242\, x_1x_7 + 0.0067874\, x_2x_3 + 0.0035249\, x_2x_4 - 0.0055574\, x_2x_5 - 0.0043812\, x_2x_6 + 0.030711\, x_2x_7 + 0.0094085\, x_3x_4 + 0.053677\, x_3x_5 + 0.0010114\, x_3x_6 - 0.053827\, x_3x_7 + 0.034271\, x_4x_5 + 0.01587\, x_4x_6 + 0.020636\, x_4x_7 + 0.045626\, x_5x_6 - 0.018408\, x_5x_7 + 0.022394\, x_6x_7 - 0.11774\, x_1^2 - 0.0036513\, x_2^2 - 0.056\, x_3^2 - 0.047269\, x_4^2 + 0.21329\, x_5^2 - 0.011558\, x_6^2 + 0.21522\, x_7^2 \quad (4)$$

3.2 VFE Multi-objective Optimization

This optimization method seeks to discover the most optimal values for both the Head Injury Criterion (HIC) and the drag coefficient (Cd), with the goal of maintaining a balanced trade-off between the efficiency of the aerodynamics and the safety of pedestrians. The optimization procedure creates a set of solutions that give the optimal values for these two objectives based on seven essential vehicle front-end design parameters. These solutions are generated by the optimization process.

Table 5 *Optimal solution obtained from multi-objective optimization*

No.	Cd	HIC Log 100	HIC	Parameters in coded matrix						
				x_1	x_2	x_3	x_4	x_5	x_6	x_7
1	0.1885	1.0456	123.3673	-0.9973	0.0732	-0.9993	0.3923	-0.2654	0.9816	-0.9938
2	0.1885	1.0456	123.3673	-0.9973	0.0732	-0.9993	0.3923	-0.2654	0.9816	-0.9938
3	0.1886	1.0414	121.0041	-0.9973	0.08	-0.9987	0.4821	-0.2774	0.9881	-0.9932
4	0.1886	1.0433	122.0675	-0.9973	0.0732	-0.9993	0.4548	-0.2654	0.9816	-0.9938
5	0.1889	1.0369	118.5223	-0.9968	0.0904	-0.9967	0.4051	-0.3044	0.9932	-0.9717
6	0.1891	1.0328	116.3054	-0.9968	0.0736	-0.9987	0.495	-0.3016	0.9866	-0.968
7	0.1894	1.027	113.2400	-0.9966	0.0971	-0.9971	0.4502	-0.3262	0.9903	-0.9458
8	0.1895	1.0243	111.8407	-0.9971	0.0807	-0.9982	0.6035	-0.2812	0.9889	-0.9573
9	0.1898	1.0176	108.4426	-0.9965	0.09	-0.9964	0.4193	-0.3069	0.9973	-0.9095
10	0.19	1.015	107.1519	-0.9961	0.0694	-0.9966	0.5889	-0.2999	0.9941	-0.9224
11	0.1903	1.0087	104.0878	-0.9965	0.1254	-0.9963	0.4856	-0.3116	0.9953	-0.8913
12	0.1903	1.0114	105.3901	-0.9942	0.0885	-0.9971	0.5664	-0.2616	0.9947	-0.9039
13	0.1904	1.0059	102.7543	-0.9966	0.088	-0.9965	0.5381	-0.2809	0.9942	-0.8829
14	0.1906	1.0026	101.2045	-0.9965	0.0889	-0.9963	0.58	-0.2809	0.9943	-0.8778
15	0.1908	0.9994	99.7241	-0.9972	0.0725	-0.9991	0.4035	-0.2691	0.9861	-0.8383
16	0.1913	0.994	97.2747	-0.9964	0.087	-0.9949	0.8688	-0.3264	0.9922	-0.9147
17	0.1914	0.9916	96.2055	-0.9963	0.1328	-0.9949	0.6218	-0.2397	0.9927	-0.8432
18	0.1915	0.988	94.6237	-0.9948	0.1108	-0.9976	0.6421	-0.3391	0.9952	-0.8399
19	0.1916	0.9848	93.2395	-0.9968	0.103	-0.9972	0.734	-0.3266	0.9944	-0.8492
20	0.1919	0.9828	92.3847	-0.9961	0.1194	-0.997	0.7761	-0.3706	0.9817	-0.8521

The possible designs obtained by the multi-objective optimization process are summarized in Table 5, where 70 combinations of the expected design parameters are displayed. However, for clarity and conciseness, only 20 representative models are listed in the table. The solutions are sorted from those with the lowest drag coefficient (Cd) values to those with the highest, with Cd values reported to four significant figures for precision.

The Cd value for the first model in the table is 0.1885, indicating superior aerodynamic performance. Although this model also features the lowest drag coefficient, at 0.098, it ironically also has the highest HIC maximum value of 123.3673, which indicates a worse likelihood of pedestrian head injury than the others in the event of an impact. The result speaks to the optimization process' trade-off between a lower drag coefficient and the safety of pedestrians.

By evaluating the array of options produced, a balance can be achieved between aerodynamic efficacy and pedestrian safety. The Pareto-optimal solutions produced by the optimization procedure facilitate a more informed judgment in selecting the most appropriate vehicle front-end design that satisfies both safety and performance standards.

Int. Journal of Integrated Engineering Vol. 18 No. 3 (2026) p. 147-165

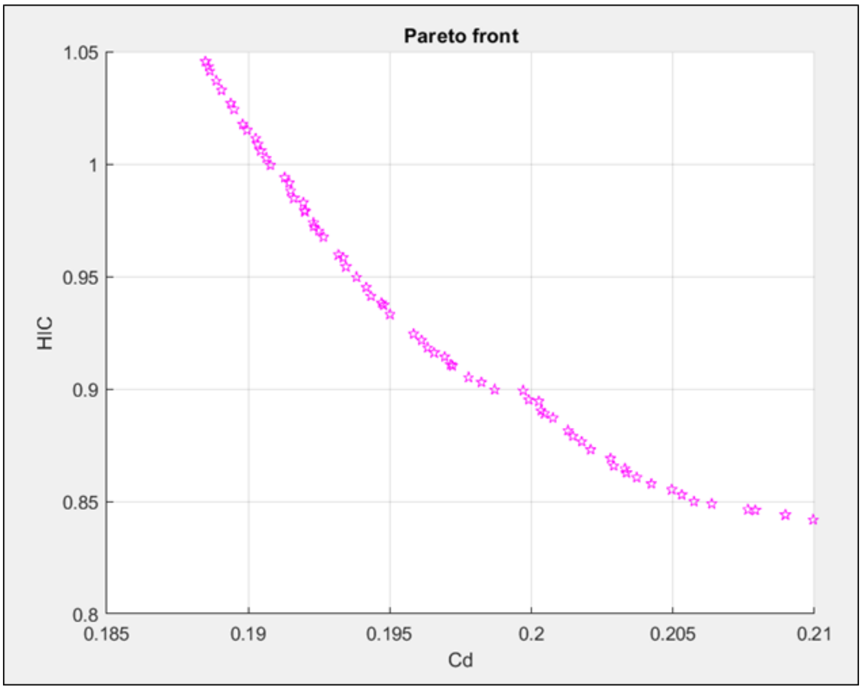

Fig. 4 *Pareto-optimal solutions for vehicle front-end design optimization*

This compromise is further demonstrated by the Pareto front graph in Figure 4, which graphically depicts the connection between Cd and HIC. The curve illustrates the compilation of Pareto-optimal solutions, indicating that enhancements in one objective, like decreasing Cd for improved aerodynamics, result in trade-offs with another objective, specifically an increase in HIC and a decrease in pedestrian safety. The graph illustrates that models exhibiting lower Cd values typically correspond to higher HIC values, highlighting the difficulty in attaining an optimal equilibrium between aerodynamic efficiency and pedestrian safety.

The Pareto front offers critical information for the decision-making process, enabling engineers to determine the optimal vehicle front-end design. Through the analysis of this trade-off, a design can be identified that adequately fulfils both performance and safety criteria while achieving a balanced optimization result.

3.2.1 Best Model Identification

Table 6 presents the coded and actual values of the key design parameters, including the windshield angle, bumper lead, and hood length. Values are coded in the CCD process, as they will be used in a mathematical modelling and optimization process where variables need to be normalized. However, when the model is to be translated into an actual design for practical purposes, exact values have to be used. This conversion of coded to uncoded data is necessary to represent the actual size, shape, or other physical property of the object being modelled.

Table 6 *Uncoded parameters for sedan model 15*

x	Parameter	Coded Value	Actual Value
x_1	Windshield Angle	-0.9972	29°
x_2	Bumper Lead	0.0725	31.45 mm
x_3	Bumper Centre Height	-0.9991	516 mm
x_4	Hood Leading Edge	0.4035	120.18 mm
x_5	Hood Length	-0.2691	841.48 mm
x_6	Hood Angle	0.9861	17.95°
x_7	Hood Edge Height	-0.8383	587.15 mm

Cd = 0.1908
HIC = 99.7241

Considering the purpose of validating the Cd value using ANSYS simulation, Model 15 retrieved from Table 5 has been selected. This model was chosen since its Head Injury Criterion (HIC) value is below 100, recognized as a safe threshold for pedestrians in a collision. As an additional point of interest, Model 15 has a Cd value of 0.1908, thus making it a good candidate for this study. Before starting to create Model 15 in the CATIA V5 Module, it is essential to convert the model parameters to a matrix of decoded numbers. This translation is critical to properly represent the size and characteristics of the physical world, which is necessary in order for detailed design and simulation.

To proceed with the design in CATIA V5, it is crucial to input the actual values of the parameters. This will ensure that the 3D model accurately represents the true size of the vehicle. Realistic physical environment representation is crucial for high-fidelity simulations. Using the original values makes sure that the model made in CATIA V5 can be used in ANSYS for validating the drag coefficient (Cd) and running crash tests to make sure pedestrians are safe. Correct representation of these values will ensure that the simulations accurately reflect the real-world scenarios, leading to reliable results with regard to aerodynamics and pedestrian safety.

3.2.2 Significant Correlating Parameters

The ANOVA study found that the factors that affect the drag coefficient (Cd) and the Head Injury Criterion (HIC) were significantly similar (p-value < 0.05). These features, along with the associated parameters of bumper centre height (x_3), hood length (x_5), and their interaction between bumper centre height and hood edge height (x_3x_7), are particularly relevant in minimizing aerodynamic drag and improving pedestrian safety. All of these elements are also among the major contributors in deciding how air moves around the car and how that car affects a pedestrian should a low speed collision occur.

Table 7 provides additional evidence for these findings by displaying the ANOVA results, which demonstrate a correlation between the factors impacting Cd and HIC.

Table 7 *ANOVA results showing correlation between drag coefficient (Cd) and Head Injury Criterion (HIC) parameters*

Drag Coefficient (Cd)			Head Injury Criterion (HIC)		
Source	F value	P value	Source	F value	Pvalue
x_1	376.83	<0.0001	**x_3**	**20.1**	**<0.0001**
x_3	**6.70**	**0.0119**	**x_5**	**83.55**	**<0.0001**
x_5	**7.77**	**0.0070**	x_2x_7	6.02	0.0169
x_7	52.62	<0.0001	x_3x_5	18.40	<0.0001
x_1x_4	4.72	0.0335	**x_3x_7**	**18.50**	**<0.0001**
x_1x_7	28.29	<0.0001	x_4x_5	7.50	0.0080
x_3x_7	**16.02**	**0.0002**	x_5^5	10.56	0.0018
x_2^2	9.33	0.0033	x_7^7	10.76	0.00017

Note: The values in bold indicate the parameters that overlap between the drag coefficient and the Head Injury Criterion (HIC) ($p < 0.05$).

3.2.2.1 Bumper Centre Height (x_3)

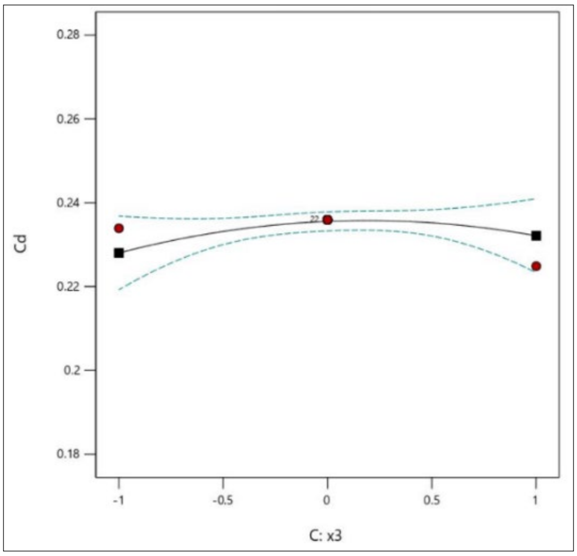

Fig. 5 *Graph of bumper centre height against Drag Coefficient (Cd)*

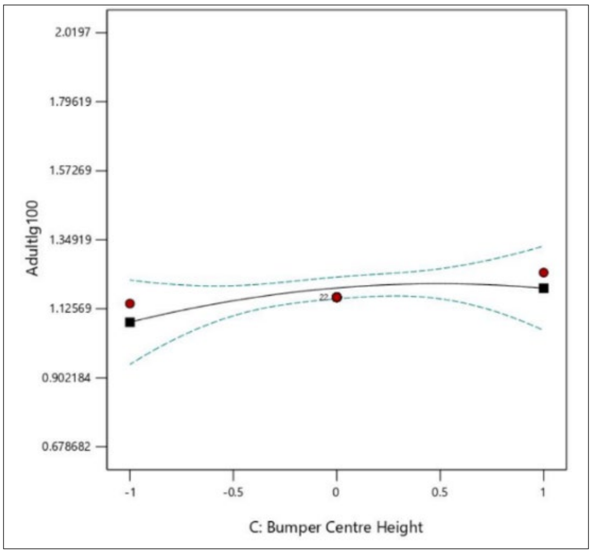

Fig. 6 *Graph of bumper centre height against Head Injury Criterion (HIC)*

The two graphs show the effect of bumper centre height (x_3) on drag coefficient (Cd) in Figure 5 as well as Head Injury Criterion (HIC) in Figure 6 and demonstrate a clear compromise between aerodynamic performance and pedestrian safety. The first graph shows that as bumper height increases, the drag coefficient experiences a slight rise, indicating a potential reduction in aerodynamic efficiency. This is due to changes in airflow around the vehicle, affecting fuel consumption or reduced speed. In a similar way, the second graph shows a slight but consistently increasing portions for HIC values as bumper height increases, indicating an increased risk of head injuries following a pedestrian impact. Even with these weaker trends, the ANOVA analysis shows that bumper height is still significant for both Cd and HIC ($p < 0.05$), emphasizing its dual role in vehicle design.

The comparison between these graphs highlights a crucial trade-off: the higher the bumper, the more aerodynamic performance but the increased potential risk of injury to a pedestrian. This is consistent with the findings of previous researchers which concluded that lower bumpers will suffer severe tibia and fibula fractures, while higher bumpers will shift the injury location to the less critical knee or ankle [7]. Subsequently, although higher bumpers may lead to lower leg injuries, they may also result in to more serious injuries to the upper body such as head injuries, which may be illustrated by the upward trend for HIC in the second graph. That creates some design challenges, as adding aerodynamic efficiency components might negatively affect pedestrian safety.

Although the differences in Cd and HIC are fairly subtle, the statistical significance indicates that even seemingly minor changes in bumper height may have some real-world effectiveness. Thus, automakers would need to optimize bumper placement to balance airflow with pedestrian protection. This work suggests the need for regulatory authorities to set more stringent bumper height standards to reduce the global severity of pedestrian injuries while keeping the functionality of vehicles. In the end, these results support the nature of the vehicle design puzzle that advancements in one area come with a sacrifice to another.

3.2.2.2 Hood Length (x_5)

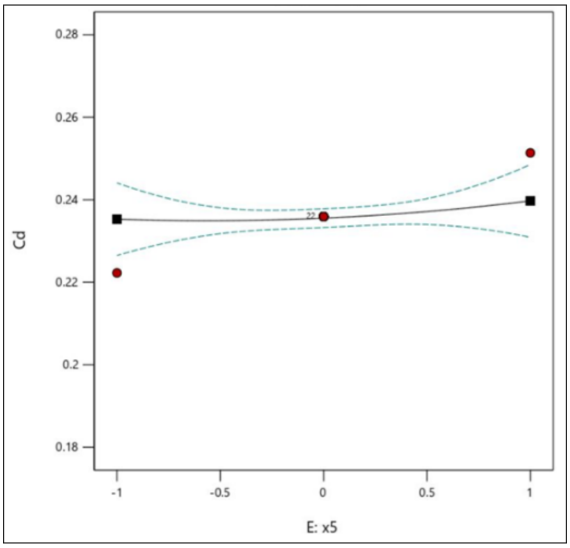

Fig. 7 *Graph of hood length against Drag Coefficient (Cd)*

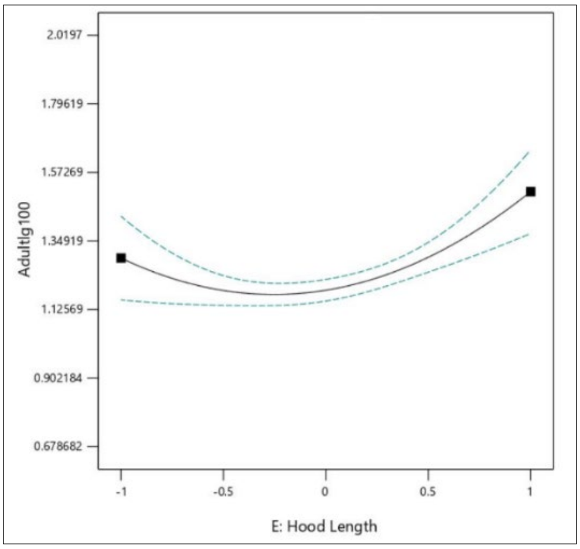

Fig. 8 *Graph of hood length against Head Injury Criterion (HIC)*

As observed from the graphs, it can be seen that hood length (x_5) has a considerable impact on drag coefficient (Cd) in Figure 7 and head injury criterion (HIC) in Figure 8. In the first graph, clearly as hood length increases, Cd increases more progressively, which likely has a detrimental effect on aerodynamics. This can be attributed to increased airflow resistance over a longer front-end surface. Next, the second graph shows that there isn't a straight line between hood length and HIC. It shows that neither short nor long hoods lower the risk of head injury. Instead, moderate hood lengths have the lowest HIC values, but excessive hood lengths lead to a rise in HIC values.

These findings correspond with Fu's research, which highlights the significance of front-end design in enhancing aerodynamic performance. Fu's work indicates that altering vehicle shape, including reducing hood height or tweaking windshield angle, can markedly decrease drag [8]. For example, decreasing the vehicle's front height diminishes airflow pressure concentration, resulting in a 6% reduction in drag, whereas angling the windshield by 3 degrees reduces airflow separation, decreasing Cd by 3%. This underscores that even little alterations to the hood and front-end geometry can significantly impact aerodynamic efficiency [8].

Comparing these findings with the graphs reveals that hood length is crucial in optimizing aerodynamics and ensuring pedestrian safety. Longer hoods may marginally diminish aerodynamic efficiency, but they also affect the intensity of pedestrian collision. Fu's research substantiates the notion that meticulous optimization of front-end design can improve aerodynamic efficiency while preserving vehicle integrity and occupant space. Consequently, car manufacturers must determine an appropriate hood length that minimizes drag while safeguarding pedestrian safety, ensuring that advancements in one domain do not inadvertently introduce problems in another.

3.2.2.3 Interaction Between Bumper Centre Height and Hood Edge Height (x_3x_7)

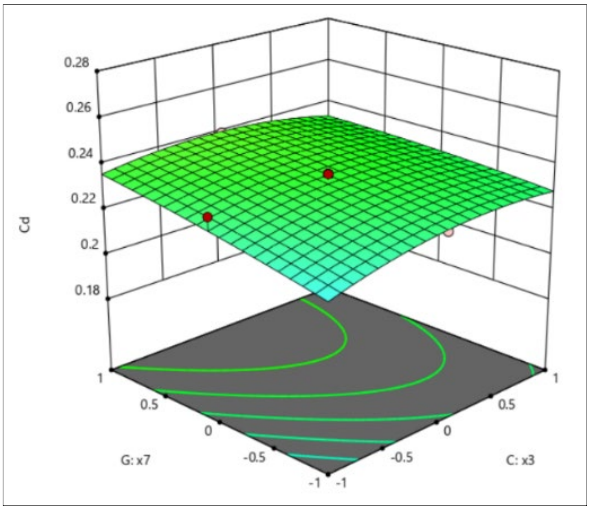

Fig. 9 *Graph of bumper centre height and hood edge height against Drag Coefficient (Cd)*

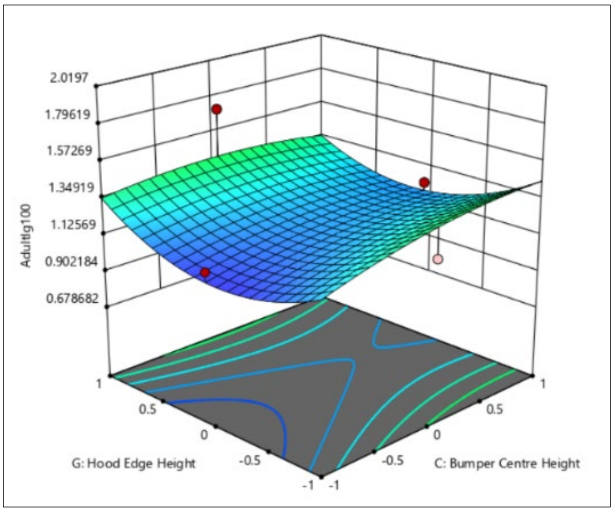

Fig. 10 *Graph of bumper centre height and hood edge height against Head Injury Criterion (HIC)*

The 3D surface plots depict the relationship between bumper centre height (x_3) and hood edge height (x_7) in affecting both the drag coefficient (Cd) and the Head Injury Criterion (HIC). These graphs illustrate the impact of alterations in vehicle front-end design on aerodynamics and pedestrian safety. The Figure 9 illustrates the correlation between Cd and the interaction between bumper centre height and hood edge height. The green mesh surface illustrates this relationship, whereas the contour map below offers a plan view of the variances. The trend indicates that reduced bumper centre heights and elevated hood edges lead to a reduction in Cd, hence enhancing aerodynamic efficiency. In contrast, elevated bumper heights and reduced hood edges result in an increase in drag coefficient (Cd), hence augmenting aerodynamic drag. This tendency corresponds with aerodynamics research indicating that alterations to front-end design might enhance airflow and diminish pressure accumulation, hence reducing drag.

The second graph in Figure 10 analyses the influence of bumper centre height and hood edge height on HIC values. The blue mesh surface illustrates the impact of parameter variations on head injury risks. Observations reveal that elevated bumper and hood edge heights correlate with increased HIC values, signifying a heightened risk of serious head injuries in pedestrian collisions. Conversely, reduced heights of bumpers and hood edges diminish HIC values, although they may elevate the risk of injuries to the lower limbs. The contour map at the base illustrates how diverse parameter combinations result in differing degrees of head injury severity.

An analysis of both graphs indicates a notable design compromise. From an aerodynamic standpoint, a reduced bumper centre height and an elevated hood edge height enhance aerodynamic performance by decreasing the drag coefficient (Cd). From a pedestrian safety perspective, an elevated bumper centre height and hood edge height augment HIC values, resulting in an increased risk of serious head injuries. These results align with prior research on car front-end design. Previous researchers underscore the impact of bumper placement on lower limb injuries, whereas stresses that elevated hood edges markedly elevate the risk of catastrophic head injuries in pedestrian collisions [15, 16].

These findings indicate significant design implications. Vehicle designers must meticulously calibrate bumper and hood edge heights to balance aerodynamics and safety, so minimizing both drag coefficient (Cd) and head injury criterion (HIC), assuring optimal efficiency while safeguarding pedestrian safety. The incorporation of energy-absorbing materials, such foam layers or deformable structures surrounding bumpers and hoods, can mitigate impact forces and lower HIC values. Furthermore, altering vehicle designs through the use of slanted hoods and optimally placed bumpers may yield a viable solution that satisfies both aerodynamic efficiency and pedestrian safety objectives.

In summary, the graphs demonstrate the significant correlation among bumper centre height, hood edge height, drag coefficient, and pedestrian injury risks. Elevated hood edges and diminished bumpers mitigate drag but exacerbate pedestrian head injury severity, necessitating meticulous trade-offs in vehicle design. These findings underscore the imperative of optimizing front-end geometry to improve efficiency and safety in car design.

3.3 Validation of Optimized Model

The initial phase in validating the improved Vehicle Front-End (VFE) design entailed creating an accurate 3D model utilizing CATIA V5R21. The refined design parameters including windshield angle, bumper lead, hood length, and hood angle were employed to generate the 3D model. These requirements guaranteed that the vehicle's front-end design was precisely depicted in the digital realm. The principal specifications comprised a windshield angle of 29 degrees, a bumper lead of 31.45 mm, a hood length of 841.48 mm, and a hood angle of 17.95 degrees. Inputting these values into CATIA V5R21 produced a realistic 3D model as shown in Figure 11 of the vehicle's front-end, accurately mirroring the actual geometry for subsequent examination.

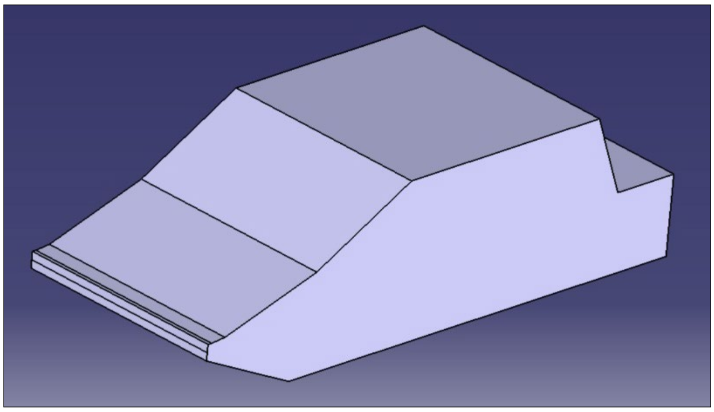

Fig. 11 *Validated 3D model in CATIA V5R21*

Following the completion of the development of the 3D model, the subsequent stage was to conduct the Computational Fluid Dynamics (CFD) analysis in ANSYS in order to evaluate the aerodynamic performance of the improved Vehicle Front-End (VFE) design. The vehicle's aerodynamic efficiency is greatly affected by the drag coefficient (Cd), which is the primary parameter that was studied. The result of Cd value in Table 8 is an important statistic for validation because it is directly related to the overall dynamics of the vehicle as well as the fuel efficiency of the vehicle.

Table 8 *ANSYS simulation results for Drag Coefficient*

x_1	29
x_2	31.45
x_3	516
x_4	120.18
x_5	841.48
x_6	17.95
x_7	587.15
Nodes	51188
Element	266440
Time	0:03:44
Iterations	94
Drag Coefficient	0.2132

The mesh that was utilized in the simulation was comprised of 51,188 nodes and 266,440 elements, with an element size of 0.5 meters. This was done to guarantee that crucial areas such as the hood, windshield, and bumper were accurately recorded. With this level of refinement, it was possible to do a comprehensive examination of the airflow around the front end of the vehicle while still preserving the efficiency of the computing process [17].

The simulation was conducted at a velocity of 50 km/h, emulating standard low-speed conditions for urban driving, pertinent to safety evaluations concerning pedestrian collisions [18]. The simulation concluded in 3 minutes and 44 seconds after 94 iterations, demonstrating that the mesh refinement and boundary conditions

Int. Journal of Integrated Engineering Vol. 18 No. 3 (2026) p. 147-165

produced a stable and precise solution without significant computing expense. The CFD analysis produced a drag coefficient (Cd) of 0.2132. This number denotes the aerodynamic efficiency of the vehicle's front-end, with reduced Cd values signifying superior streamlined performance.

The mesh refinement, employing a 0.5m element size, guaranteed that the key regions, where intricate flow phenomena like turbulence arise, were adequately detailed to accurately represent the airflow dynamics [19]. The rapid convergence of the simulation within 94 iterations indicates that the solver was successful in obtaining a stable solution. The drag coefficient derived from the simulation closely matches the target established throughout the optimization phase, validating the successful implementation of aerodynamic design enhancements.

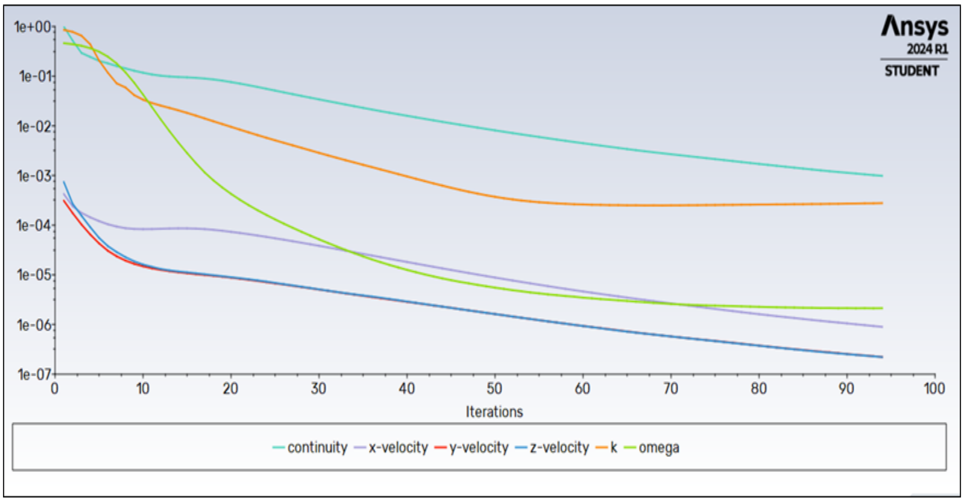

Fig. 12 *Residual convergence plot for ANSYS simulation*

Alongside the drag coefficient study, the convergence history from the ANSYS simulation offers critical insights into the stability and reliability of the computational outcomes. The graph in Figure 12 depicts the residuals for multiple parameters—continuity, x-velocity, y-velocity, z-velocity, turbulence kinetic energy (k), and omega—across 100 iterations.

The graphic demonstrates that all parameters display a declining trend in their residuals, signifying that the simulation was effectively converging towards a stable solution. The residuals for continuity and velocity components markedly diminished during the initial iterations, indicating rapid stabilization of the flow field. The swift decline in these values indicates that the mesh and boundary conditions were correctly established, resulting in effective convergence [20].

Over the course of the 100 iterations, the residuals for both the x-velocity and the y-velocity fell to around $1e^{-6}$ and $1e^{-7}$ respectively. This is well within the permitted limits for computational fluid dynamics (CFD) simulations. Convergence towards low residuals was also demonstrated by the turbulence model parameters, such as k and omega, which further serves to validate the dependability of the turbulence model that was utilized in the simulation.

The convergence behaviour increases confidence in the drag coefficient (Cd) estimate of 0.2132 derived from the simulation. The stability observed in the residuals signifies that the numerical solution is dependable and precisely depicts the physical occurrences surrounding the vehicle's front-end. The convergence history not only corroborates the drag coefficient result but also highlights the efficacy of the simulation configuration and the quality of the mesh utilized in the ANSYS study.

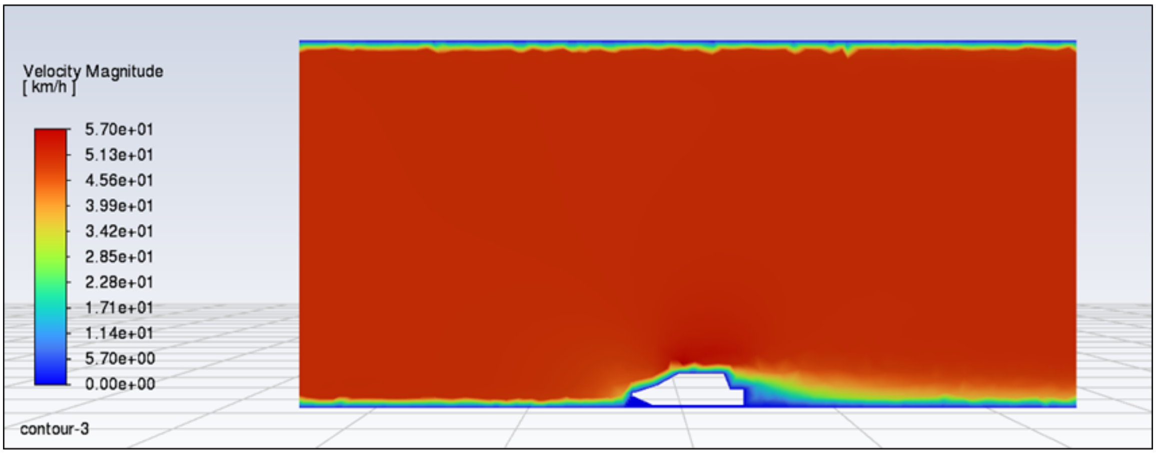

Fig. 13 *Velocity contour for ANSYS simulation*

The velocity magnitude distribution from the ANSYS simulation elucidates the aerodynamic behaviour surrounding the optimised Vehicle Front-End (VFE) design. The visualisation illustrates flow patterns and velocity magnitudes, demonstrating the design's efficacy in minimising drag and optimising airflow.

Figure 13 displays a colour gradient denoting velocity magnitude in kilometres per hour (km/h), with blue representing lower velocities and red indicating higher velocities. The simulation indicates a maximum velocity of 57 km/h, accompanied by a significant decrease in velocity behind the vehicle. A significant high-velocity area at the forefront (shown in red) underscores the efficacy of the optimised VFE design in directing airflow, resulting in a streamlined configuration that reduces turbulence and drag [21].

The visualisation demonstrates streamlined airflow over the leading edges of the VFE, exhibiting minimum separation at crucial locations such as the hood and windscreen. This aerodynamic characteristic is essential for attaining a low drag coefficient (Cd) of 0.2132, signifying less airflow resistance. The velocity gradient along the sidewalls indicates that airflow adheres to the vehicle's surface across a greater distance, enhancing aerodynamic stability [22].

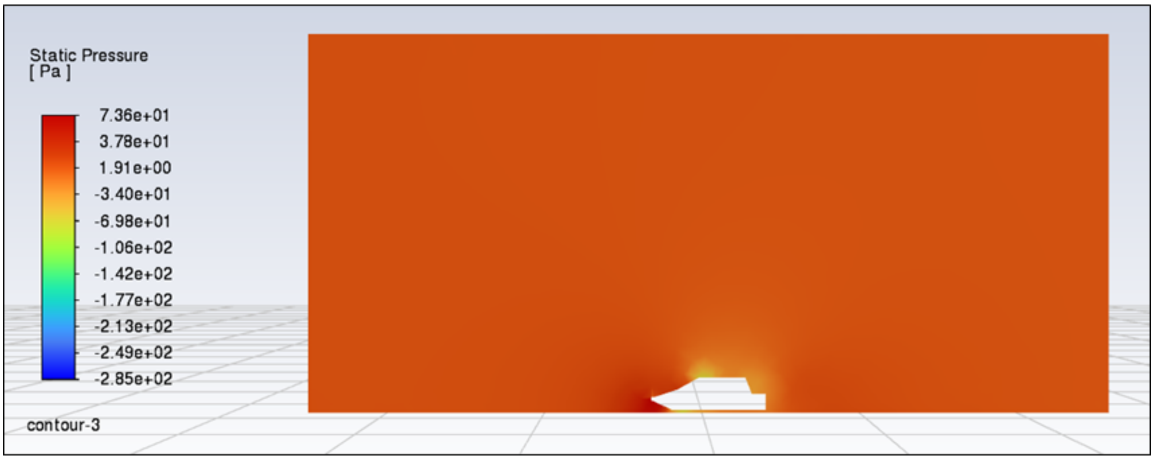

Fig. 13 *Pressure contour for ANSYS simulation*

The pressure contour from the ANSYS simulation demonstrates the static pressure distribution surrounding the Vehicle Front-End (VFE) design. The colour gradient signifies varying pressure levels, with red denoting high-pressure areas and blue suggesting low-pressure parts. The highest static pressure recorded in the simulation is 73.6 Pa, occurring at the stagnation point when airflow directly strikes the vehicle's front surface.

At the front end of the vehicle, air decelerates upon impact, resulting in a pressure accumulation that produces the maximum static pressure in this area. This is a natural aerodynamic phenomenon, since the incoming airflow is compelled to decelerate and compress prior to being redirected around the vehicle. This regulated pressure distribution is essential for optimising airflow efficiency, reducing unnecessary resistance, and maintaining a streamlined aerodynamic profile.

As airflow traverses the vehicle's surface, static pressure progressively diminishes, creating a seamless transition that inhibits sudden flow separation. This pressure gradient guarantees attached airflow, minimising turbulence and aerodynamic drag. Furthermore, a low-pressure zone exists beneath the vehicle due to air acceleration, potentially resulting in wake development. The optimised VFE design efficiently regulates airflow, diminishes turbulence, and enhances aerodynamic stability.

The pressure distribution indicates that the VFE design effectively regulates airflow, minimising drags and improving aerodynamic efficiency, as evidenced by the 73.6 Pa stagnation pressure, which reflects efficient pressure distribution and airflow redirection.

Through the analysis of velocity magnitude and static pressure, we can affirm that the design decisions made during the optimization process specifically, the windshield angle of 29 degrees and the bumper lead of 31.45 mm successfully contribute to the attainment of the desired aerodynamic performance. The refined shape aids in sustaining an advantageous airflow path, essential for enhancing fuel efficiency and ensuring compliance with pedestrian safety regulations.

In result, the distribution of velocity magnitude supports the results from the drag coefficient analysis and convergence history, together illustrating the effectiveness of the optimization process. The findings demonstrate that the design enhancements effectively strike a balance between aerodynamic efficiency and safety, establishing a foundation for additional refinements and validations in upcoming iterations of the VFE design.

To confirm the aerodynamic performance of the optimized Vehicle Front-End (VFE) model, it was essential to evaluate the precision of the ANSYS simulation results by determining the percentage error between the observed drag coefficient ($V_{observed}$) and the optimized target value (V_{true}). A drag coefficient of 0.1908 was chosen as the target value after running the MATLAB multi-objective optimization procedure. As a counterpoint, 0.2132 was the observed drag coefficient as determined by the ANSYS simulation.
The formula for calculating the percentage error is as follows:

$$Percentage\ error = \left|\frac{V_{observed} - V_{true}}{V_{true}}\right| \times 100 \tag{5}$$

Substituting the observed and target values into this equation yields:

$$Percentage\ error = \left|\frac{0.2132 - 0.1908}{0.1908}\right| \times 100 \tag{6}$$

Calculating this, we find:

$$Percentage\ error = \left|\frac{0.0224}{0.1908}\right| \times 100 = 11.74\% \tag{7}$$

The percentage error of about 11.74% signifies a divergence from the target value; however, it stays within a permissible range for engineering tolerances. Although the percentage error is slightly above 10%, the difference between $V_{observed}$ (0.2132) and V_{true} (0.1908) is merely 0.0224, indicating a small difference and underscoring the overall accuracy of the simulation. The percentage deviation remains acceptable, as CFD derived drag coefficients within ±10–15% of experimental values are generally considered within the allowable range due to inherent modelling and discretization uncertainties [23]. The proximity of the observed drag coefficient to the optimized target further indicates that the ANSYS simulation effectively captures the aerodynamic characteristics of the VFE design.

The validation is important as it verifies that the design enhancements implemented during the optimisation process have successfully improved the vehicle's aerodynamic efficiency. Although the drag coefficient that was measured is somewhat greater than the target, this can be ascribed to a few different causes. Some of these factors include the intricacy of the airflow around the front end of the vehicle, minor differences in mesh quality, and the inherent limits of the simulation model.

The calculated percentage error confirms the dependability of the simulation results and highlights the efficacy of the employed optimisation approaches. Notwithstanding the little divergence, the aerodynamic performance attained by the optimised design satisfies the performance objectives established in the project's earliest phases.

Moreover, the correlation between the measured drag coefficient and the desired value demonstrates that the VFE design enhances fuel efficiency and is crucial for pedestrian safety in low-speed collisions. This equilibrium is essential, as attaining minimal drag while preserving structural integrity during a collision is a fundamental goal of the vehicle's front-end design [24].

In summary, the examination of percentage error, along with insights from velocity magnitude distributions, drag coefficient evaluations, and convergence history, jointly substantiates the efficacy of the optimised VFE design. The positive association between the simulation outcomes and the optimisation objectives establishes a robust basis for subsequent refinement and iterative enhancements in future design stages. This comprehensive validation method guarantees that aerodynamic performance and safety standards are prioritised in the vehicle front-end development.

4. Conclusion

This paper illustrates the efficacy of a genetic algorithm-driven multi-objective optimization method for vehicle front-end (VFE) design, focusing on the dual objectives of reducing the drag coefficient (Cd) and improving pedestrian safety as quantified by the Head Injury Criterion (HIC). The optimization method, executed in MATLAB using the Solver-Based Optimize Live Editor Task, effectively produced a collection of Pareto-optimal solutions, achieving a compromise between aerodynamic efficiency and safety performance. The integration of computational fluid dynamics (CFD) simulations with genetic algorithms resulted in a notable decrease in drag (Cd = 0.2132) and enhanced pedestrian impact safety. This demonstrates the capability of genetic algorithms to address complex, non-linear challenges in vehicle design, particularly when balancing opposing objectives such as aerodynamics and safety.

Verification of the optimized designs through ANSYS simulations confirms that the solutions are both theoretically robust and practically viable. The study's findings advance efforts in the automotive industry to develop vehicles that comply with regulatory standards for fuel efficiency and pedestrian safety. As regulations become increasingly stringent regarding environmental and safety standards, this study underscores an effective approach to enhance front-end designs for modern automobiles.

The study also highlights practical implications for vehicle design, emphasizing the need to optimize bumper center height and hood edge height to balance aerodynamic performance and pedestrian safety. Furthermore, these findings provide supporting evidence for regulatory considerations, such as stricter bumper height standards, to reduce pedestrian injury severity while maintaining vehicle performance.

For future work, several avenues can enhance the robustness and applicability of the findings:

1. Expand Injury Metrics: Incorporate additional injury criteria (e.g., lower-body injuries such as tibia force) for a more comprehensive safety evaluation.
2. Improve Validation Accuracy: Refine CFD mesh resolution and turbulence modeling (e.g., LES) to reduce error margins.
3. Statistical Transparency: Address any anomalies in ANOVA results and explore advanced sensitivity analysis techniques, such as Sobol indices.
4. Real-World Testing: Validate computational results through physical crash tests and wind tunnel experiments.

Overall, this study demonstrates a systematic, multi-objective approach for optimizing vehicle front-end design, providing actionable insights for automotive engineers while highlighting pathways for further research to improve both aerodynamic efficiency and pedestrian safety.

Acknowledgement

The authors would like to acknowledge the support of the College of Engineering, Universiti Teknologi MARA and Institute of Postgraduate Studies for providing the facilities and financial support for this research.

Conflict of Interest

Authors declare that there is no conflict of interests regarding the publication of the paper.

Author Contribution

The authors confirm their contribution to the paper as follows: ***study conception and design:*** *Author A.N., Author K.V.;* ***data collection:*** *Author A.N.;* ***analysis and interpretation of results:*** *Author A.N., Author K.V., Author S.S.;* ***draft manuscript preparation:*** *Author A.N., Author K.V., Author S.S. All authors reviewed the results and approved the final version of the manuscript.*

References

[1] World Health Organization. (2009). *Global Status Report on Road Safety: Time for Action*. World Health Organization.

[2] Ministry of Transport Malaysia. (2019). "Malaysia Road Fatalities Index,".

[3] B. Griffin, K. Watt, B. Wallis, L. Shields, and R. Kimble. (2011). "Paediatric low speed vehicle run-over fatalities in Queensland," *Injury Prevention*, vol. 17, no. SUPPL. 1. https://doi.org/10.1136/ip.2010.030304

[4] X. Liu and J. Yang. (2003). "Effects of Vehicle Impact Velocity and Front-End Structure on the Dynamic Responses of Child Pedestrians".

[5] Y. Peng, C. Deck, J. Yang, D. Otte, and R. Willinger. (2013). "A Study of Adult Pedestrian Head Impact Conditions and Injury Risks in Passenger Car Collisions Based on Real-World Accident Data," *Traffic Inj Prev*, vol. 14, no. 6, pp. 639–646. https://doi.org/10.1080/15389588.2012.733841

[6] C. Gao. (2023). "Effect of front windshield angle on drag coefficient of electric vehicles," *Theoretical and Natural Science*, vol. 12, no. 1, pp. 101–107. https://doi.org/10.54254/2753-8818/12/20230442

[7] D. Otte and Haasper. (2007). Characteristics on Fractures of Tibia and Fibula in Car Impacts to Pedestrians and Bicyclists-Influences of Car Bumper Height and Shape".

[8] Y. Fu. (2023). "Aerodynamics and Drag of a Car".

[9] V. Kausalyah, S. Shasthri, K. A. Abdullah, M. M. Idres, Q. H. Shah, and S. V. Wong. (2014). "Optimisation of vehicle front-end geometry for adult and pediatric pedestrian protection," *International Journal of Crashworthiness*, vol. 19, no. 2, pp. 153–160. https://doi.org/10.1080/13588265.2013.879506

[10] Y. Mizuno. (2005). "Summary of IHRA Pedestrian Safety WG Activities (2005)-Proposed Test Methods To Evaluate Pedestrian Protection Afforded By Passenger Cars".

[11] P. Bajpai. (2010). "Genetic Algorithm-an Approach to Solve Global Optimization Problems".

[12] Y. D. Shahakar, Dr. A. S. Telang, and D. A. Shahakar. (2022). "Introduction to Optimization Toolbox in MATLAB to Optimize Different Types of Optimization Problem," *International Journal of Scientific Research in Engineering and Management*, vol. 06, no. 04. https://doi.org/10.55041/ijsrem12155

[13] S. N. Tung, J. B. Jaafar, I. A. Aziz, H. G. Nguyen, and A. N. Bui. (2021). "Genetic Algorithm for Solving Multi-Objective Optimization in Examination Timetabling Problem," *International Journal of Emerging Technologies in Learning*, vol. 16, no. 11, pp. 4–24. https://doi.org/10.3991/ijet.v16i11.21017

[14] Willmott Cort J. and Matsuura Kenji. (2005). "Advantages of the mean absolute error (MAE) over the root mean square error (RMSE) in assessing average model performance".

[15] Insurance Institute for Highway Safety and Highway Loss Data Institute. (2023). "Vehicles with higher, more vertical front ends pose greater risk to pedestrians".

[16] Y. Matsui, M. Hitosugi, and K. Mizuno. (2011). "Severity of vehicle bumper location in vehicle-to-pedestrian impact accidents," *Forensic Sci Int*, vol. 212, no. 1–3, pp. 205–209. https://doi.org/10.1016/j.forsciint.2011.06.012

[17] A. Lintermann. (2021). "Computational Meshing for CFD Simulations,"pp. 85–115. https://doi.org/10.1007/978-981-15-6716-2_6

[18] V. Branzi, L. Domenichini, and F. La Torre. (2017). "Drivers' speed behaviour in real and simulated urban roads – A validation study," *Transp Res Part F Traffic Psychol Behav*, vol. 49, pp. 1–17. https://doi.org/10.1016/j.trf.2017.06.001

[19] K. L. Nabutola and S. K. S. Boetcher. (2021). "On the Validation of Turbulence Models for Wheel and Wheelhouse Aerodynamics," *J Verif Valid Uncertain Quantif*, vol. 6, no. 2. https://doi.org/10.1115/1.4050611

[20] J. Tu, G.-H. Yeoh, and C. Liu. (2018). "CFD Solution Analysis: Essentials," in *Computational Fluid Dynamics*, Elsevier, pp. 211–253. https://doi.org/10.1016/b978-0-08-101127-0.00006-4

[21] Z. Xia and M. Huang. (2024). "Optimizing the Aerodynamic Efficiency of Electric Vehicles via Streamlined Design: A Computational Fluid Dynamics Approach," *International Journal of Heat and Technology*, vol. 42, no. 3, pp. 865–876. https://doi.org/10.18280/ijht.420315

[22] Y. Liao, K. Cheng, W. Sun, Y. Zhao, X. Jia, and W. Qi. (2024). "Computational fluid dynamics analysis of aerodynamic characteristics in long-endurance unmanned aerial vehicles," *Heliyon*, vol. 10, no. 19. https://doi.org/10.1016/j.heliyon.2024.e38804

[23] Katz, J. (2016). *Automotive aerodynamics*. John Wiley & Sons.

[24] E. Mirmahdi and A. Khoubrou. (2021). "The Effect of Aerodynamic Forces on Automotive Design and Reducing Fuel Consumption". https://doi.org/10.37628/ijra